Journal of Solid State Chemistry 184 (2011) 2987–2993

Contents lists available at SciVerse ScienceDirect

Journal of Solid State Chemistry

journal homepage: www.elsevier.com/locate/jssc

The ferroelectric phase of $CdTiO_3$: A powder neutron diffraction study

Brendan J. Kennedy [a,*], Qingdi Zhou [a], Maxim Avdeev [b]

[a] School of Chemistry, The University of Sydney, Sydney, NSW 2006, Australia
[b] Bragg Institute, Australian Nuclear Science and Technology Organisation, Private Mail Bag 1, Menai, NSW 2234, Australia

ARTICLE INFO

Article history:
Received 4 June 2011
Received in revised form
4 August 2011
Accepted 22 August 2011
Available online 31 August 2011

Keywords:
Illmenite–perovskite transition
Neutron diffraction
^{114}Cd
Ferroelectric

ABSTRACT

The synthesis of bulk samples of polycrystalline $CdTiO_3$ in both the rhombohedral ilmenite and orthorhombic perovskite forms is described and the structures of these have been refined using powder neutron diffraction data. This involved the preparation of samples enriched in ^{114}Cd. Cooling perovskite-type $CdTiO_3$ to 4 K induces a ferroelectric phase transition, with the neutron data suggesting the low temperature structure is in $Pna2_1$. Mode analysis shows the polar mode to be dominant at low temperatures. The ilmenite-structure of $CdTiO_3$ is compared with that of $ZnTiO_3$. The refined scattering length of the ^{114}Cd is estimated to be 5.56 fm. Attempts to dope $CdTiO_3$ with Ca and Sr are described.

1. Introduction

Cadmium titanate ($CdTiO_3$) is somewhat of an enigma in solid state chemistry, and is relatively poorly studied, partially due to the toxicity of cadmium and partially due to difficulties in obtaining pure $CdTiO_3$ since it has only a moderate stability with respect to the oxides [1]. $CdTiO_3$, like $CdSnO_3$ [2] can be synthesised with either an ilmenite or perovskite type structure. Recently Wang and co-workers reported the preparation of a hexagonal phase using sol–gel methods, although the precise structure of this is unknown [3]. The ilmenite-like phase of $CdTiO_3$ is unstable at high temperatures and, as was first experimentally demonstrated by Posnjak and Barth [4], undergoes an irreversible reconstructive phase transition to the perovskite phase near 900 °C. The perovskite phase decomposes, through the loss of Cd, if heated to ~1000 °C. In recent years, there has been growing interest developing thin films of cadmium oxides for a variety of uses including as a photocatalyst [5].

There has been some uncertainty regarding the precise structure of the perovskite phase of $CdTiO_3$. This is a consequence of the combination of its ferroelectric properties [6] and the subtleties in the various octahedral tilting schemes observed for perovskites [7]. Kay and Miles [8] proposed a ferroelectric structure for $CdTiO_3$ at room temperature in space group $Pc2_1n$ (an alternate setting of space group 33, $Pna2_1$), whereas Sasaki et al. [9] concluded it was non-polar in *Pbnm* (SG 62), and hence isostructural with $CaTiO_3$ [10]. Subsequently it was demonstrated that $CdTiO_3$ undergoes a displacive ferroelectric phase transition at about 80 K [6], with recent X-ray studies suggesting the low temperature ferroelectric phase is in $Pna2_1$ [6] or $P2_1ma$ [11] while the room temperature paraelectric phase is in *Pbnm*. The structure of the ferroelectric phase of $CdTiO_3$ is of interest since the TiO_6 octahedron is well known for its tendency to form polar groups where the Ti position is off centred with respect to the geometrical centre of the surrounding oxygen atoms. Such polar structures exist in compounds such as $PbTiO_3$ [12], $BaTiO_3$ [13] and others [14]. Competition with octahedral rotation [15] in the orthorhombic phase of $CaTiO_3$ appears to suppress the off-centring. Dielectric measurements have suggested that $CaTiO_3$ is an incipient ferroelectric similar to $SrTiO_3$ at low temperatures [16].

In the present work we have used high resolution neutron diffraction methods to refine the structure of the three phases of $CdTiO_3$, namely the paraelectric ilmenite and perovskite phases and the ferroelectric perovskite phase. It is expected that neutron diffraction will provide a more accurate and precise description of these structures compared with X-ray diffraction methods due to the presence of the heavy Cd cations. To circumvent the high neutron absorption cross section of naturally occurring Cd we used samples enriched in ^{114}Cd.

2. Experimental

Synthesis: *$CdTiO_3$* ^{114}CdO (~0.7 g) (Isoflex 99.8% isotope purity) was used as supplied and TiO_2 (Aldrich 99.9+%) was preheated at 1000 °C for 12 h before use. The two oxides were mixed by hand and heated at 700 °C for 12 h. After regrinding the powder sample were pressed into a pellet and heated at 800 °C for 60 h. The sample was heated at 950 °C for 45 h after first neutron data been

* Corresponding author. Fax: +61 2 9351 3329.
E-mail address: b.kennedy@chem.usyd.edu.au (B.J. Kennedy).

0022-4596/$ - see front matter © 2011 Elsevier Inc. All rights reserved.
doi:10.1016/j.jssc.2011.08.028

collected. Ca doped samples were prepared under similar conditions using normal CdO (Aldrich 99.99%) and $CaCO_3$ (Aldrich 99.995%) as starting materials.

$ZnTiO_3$: ZnO (Aldrich 99.9%) and TiO_2 (Aldrich 99.9+%) were preheated at 1000 °C for 12 h before use. A stoichiometric mixture of the two oxides was finely ground together by hand and heated at 700 °C for 12 h. After regrinding the powder sample were pressed into a pellet and heated at 800 °C for 60 h and then 850 °C for 20 h.

The sample was sealed in a 6 mm diameter vanadium can and neutron powder diffraction data were obtained using the high resolution powder diffractometer Echidna at ANSTO's OPAL facility at Lucas Heights [17]. The wavelength of the incident neutrons, obtained using a Ge 335 monochromator, was 1.622 Å as determined using data collected for a certified NIST SRM676 Al_2O_3 standard. This instrument has a maximum resolution of $\Delta d/d \sim 1 \times 10^{-3}$, with data collection taking around 8 h. An additional pattern was recorded for $CdTiO_3$ at 4 K using 2.442 Å neutrons. For the low temperature measurements the sample was contained in the same cylindrical vanadium can which was mounted in a closed cycle helium refrigerator.

Powder X-ray diffraction data were collected over the range $15^\circ \le 2\theta \le 90^\circ$ on a PANalytical X'Pert PRO X-ray diffractometer using Cu $K\alpha$ radiation and a PIXcel solid-state detector. Data were recorded for the three samples $Ca_{0.25}Cd_{0.75}TiO_3$, $Ca_{0.5}Cd_{0.5}TiO_3$ and $Ca_{0.75}Cd_{0.25}TiO_3$ at temperatures of up to 900 °C using an XRK 900 Reactor Chamber, operating under a vacuum of 10^{-3} Torr. The sample was allowed to equilibrate for 5 min after reaching each measurement temperature. Each pattern took around 15 min to collect.

The structures were refined using the Rietveld method implemented in the program GSAS [18,19]. The neutron peak shape was modelled by a pseudo-Voigt function and the background was estimated using an eight-term shifted Chebyschev function. Anisotropic displacement parameters were refined where possible. The neutron scattering length of ^{114}Cd was refined during the Rietveld analysis.

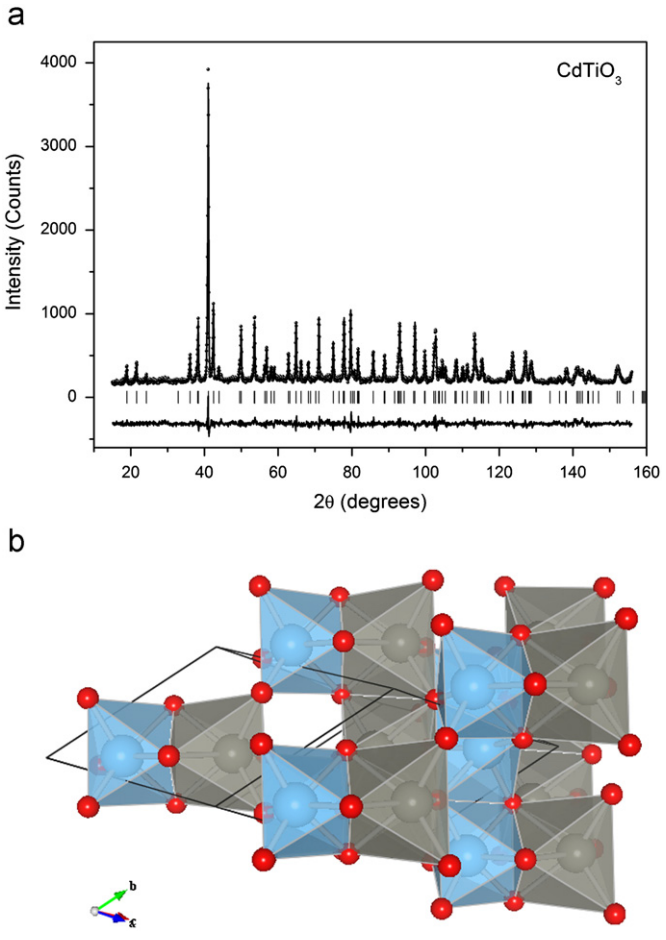

Fig. 1. (a) Observed calculated and difference neutron diffraction profiles for ilmenite-type $CdTiO_3$ refined in space group $R\bar{3}$. (b) The structure of $CdTiO_3$ is illustrated with the TiO_6 and CdO_6 represented by the blue and grey octahedron, respectively. (For interpretation of the references to colour in this figure legend, the reader is referred to the web version of this article.)

3. Results and discussion

3.1. Synthesis

The synthesis of phase pure $CdTiO_3$ is complicated by the first order nature of the ilmenite to perovskite phase transformation

Table 1
Crystal structure data and refined atomic coordinates and atomic displacement parameters (multiplied by 100.0) for $CdTiO_3$ at room temperature.

Name	Site	x	y	z	Ue × 100	
Cd	2*c*	0.3639(3)	0.3639(3)	0.3639(3)	0.95*	
Ti	2*c*	0.1509(3)	0.1509(3)	0.1509(3)	0.36*	
O	6*f*	0.5615(6)	−0.0364(4)	0.1953(4)	1.23*	
	U_{11}	U_{22}	U_{33}	U_{12}	U_{13}	U_{23}
Cd	0.61(10)	0.61(10)	0.61(10)	−0.07(6)	−0.07(6)	−0.07(6)
Ti	0.30(11)	0.30(11)	0.30(11)	−0.09(7)	−0.09(7)	−0.09(7)
O	0.88(8)	1.33(9)	1.32(9)	−0.28(8)	−0.29(9)	−0.76(8)

Table 2
Crystal structure data and refined atomic coordinates and atomic displacement parameters (multiplied by 100.0) for $ZnTiO_3$ at room temperature.

Name	Site	x	y	z	Ue × 100	
Zn	2*c*	0.3614(2)	0.3614(2)	0.3614(2)	1.30*	
Ti	2*c*	0.1466(3)	0.1466(3)	0.1466(3)	0.91*	
O	6*f*	0.5619(4)	−0.0490(3)	0.2231(3)	1.15*	
	U_{11}	U_{22}	U_{33}	U_{12}	U_{13}	U_{23}
Zn	1.32(7)	1.32(7)	1.32(7)	−0.51(5)	−0.51(5)	−0.51(5)
Ti	1.03(8)	1.03(8)	1.03(8)	−0.45(6)	−0.45(6)	−0.45(6)
O	1.12(8)	1.10(8)	1.05(8)	−0.19(6)	−0.47(7)	−0.44(7)

Table 3
Selected interatomic distances and angles in the ilmenite type structures of $CdTiO_3$ and $ZnTiO_3$.

	$CdTiO_3$	$ZnTiO_3$
a (Å)	5.80268(13)	5.49270(9)
α (deg.)	53.7041(8)	55.0831(7)
Vol (Å^3)	117.818(5)	103.777(3)
Cd–O × 3 (Å)	2.424(5) × 3	2.244(3) × 3
Cd–O × 3 (Å)	2.219(2) × 3	2.030(2) × 3
Ti–O × 3 (Å)	2.063(4) × 3	2.076(3) × 3
Ti–O × 3 (Å)	1.887(4) × 3	1.875(2) × 3
Ti–O–Ti (deg.)	101.60(10)	98.05(8)
M–O–*M* (deg.)	85.64(8)	90.37(6)
M–*M* (Å)	3.160(3)	3.035(1)
M–Ti (Å)	3.164(8)	2.993(6)
M–*M* (Å)	3.063(2)	2.986(2)
BVS *M*	1.71	1.71
BVS Ti	4.00	4.03

and by the decomposition of $CdTiO_3$ at high temperatures. The latter occurs via the formation of volatile cadmium oxides and given the toxicity of Cd presents a potential health hazard. In the present work we established it was possible to prepare gram quantities of phase pure $CdTiO_3$ in both structural forms using conventional solid state methods, provided the temperature was carefully controlled. Pure ilmenite-type $CdTiO_3$ was formed by the direct reaction of TiO_2 and CdO at a maximum temperature of 850 °C. This could be converted to the perovskite phase by heating at 950 °C for 45 h. Careful control of the heating regime allowed high quality samples of $CdTiO_3$ in both structural types to be prepared at atmospheric pressure. Liebermann [20] has demonstrated that the ilmenite phase can be stabilised through the use of pressure. Alternatively it has been demonstrated that the target phases can be prepared using sol–gel methods [21,22], however we preferred direct reaction of the oxides due to the cost of the ^{114}Cd.

Likewise care is required during the synthesis of $ZnTiO_3$. Although $ZnTiO_3$ is readily formed from a stoichiometric mixture of ZnO and TiO_2 heating it 1000 °C or higher for extended periods of time results in decomposition to a mixture of Zn_2TiO_4 and TiO_2 [23,24].

3.2. Rhombohedral structure

The powder neutron diffraction data for the ilmenite phase of $CdTiO_3$ at room temperature are shown in Fig. 1. All the observed peaks could be accounted for by a model in space group $R\bar{3}$ (Space Group 148) where the primitive unit cell contains two formula units of $CdTiO_3$. Compared to the profile of, isostructural, $ZnTiO_3$ recorded under identical conditions the pattern for $CdTiO_3$ shows a somewhat higher and more structured background. This is believed to be a consequence of both the relatively small amount of sample available for the work and incoherent scattering from the Cd. Although the scattering length of ^{114}Cd has been tabulated as 7.5 fm [25], the use of this resulted in higher than anticipated displacement parameters for the Cd cation and negative values for the Ti cation. Treating the scattering length of Cd as a variable in the refinement resulted in an improved fit $\chi^2 = 1.44$ vs 1.73 and more reasonable displacement parameters, see Table 1. A similar situation occurred for the perovskite phase of $CdTiO_3$ where the refined scattering length for the Cd was found to be 5.63(7) fm compared to the value of 5.48(8) fm for the ilmenite phase. This

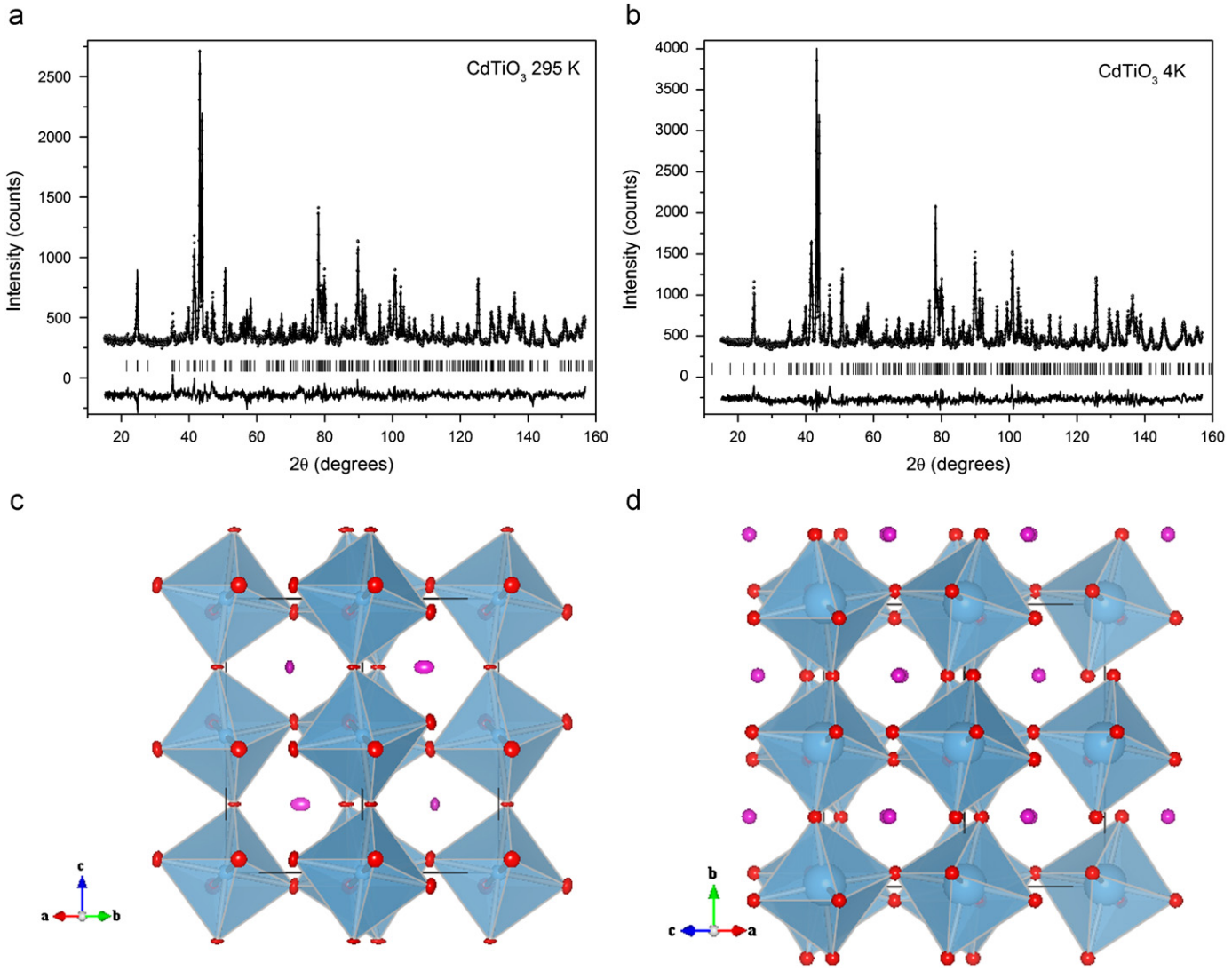

Fig. 2. Observed calculated and difference neutron diffraction profiles for perovskite-type $CdTiO_3$ refined in (a) space group *Pbnm* at 295 K and (b) $Pn2_1a$ at 4 K. The structure at 295 K is shown in (c) and that at 4 K in (d). In both cases the TiO_6 are represented by the blue octahedron. (For interpretation of the references to colour in this figure legend, the reader is referred to the web version of this article.)

value presumably reflects the precise isotopic composition of the sample used in this work (Table 2).

The refined structure of $CdTiO_3$ is unexceptional and is compared to that of $ZnTiO_3$ in Table 3. The ilmenite structure can be described as a hexagonal close-packed array of oxygen ions with metal ions occupying two-thirds of the octahedral holes. The different metal ions are in alternating layers such that each octahedron containing a cadmium (or Zn) ion shares a face with a titanium octahedron above or below it (but not both) and also shares edges with three other cadmium octahedra in the same layer. The titanium octahedra have similar linkages. The octahedral holes of the oxygen array are linked by face-sharing into chains that are filled in the sequence vacancy–Cd–Ti–vacancy–Ti–Cd–vacancy, etc. Replacement of Cd (ionic radius 0.95 Å [26]) by the smaller Zn cation (0.740 Å) results in a contraction of the cell and in the various metal–metal separations, see Table 3. The *M*–Ti distance across the face sharing octahedra is slightly longer the edge sharing, *M*–*M* or Ti–Ti distances in both $CdTiO_3$ and $ZnTiO_3$. While the average Cd–O distance is noticeably larger than the average Zn–O distance, the average Ti–O distances in the two structures are essentially the same. The Bond Valence Sums for the Ti cations in both structures are consistent with their nominal valences, whereas both the Cd and Zn are noticeably underbonded, each having a BVS of 1.71.

3.3. Orthorhombic structure

The neutron pattern for the perovskite structure of $CdTiO_3$, recorded at room temperature (Fig. 2), was well fitted in space group *Pbnm* with $a=5.3069(1)$, $b=5.4224(1)$ and $c=7.6200(2)$ Å in excellent agreement with the lattice parameters reported by Sasaki et al. [9]. This corresponds to a $\sqrt{2}a_p \times \sqrt{2}a_p \times 2a_p$ supercell of the basic cubic perovskite subcell where a_p is the idealised perovskite lattice parameter ~3.8 Å as a consequence of the cooperative tilting of the corner sharing TiO_6 octahedra. The unit cell contains four formula units of $CdTiO_3$. Space group *Pbnm* is derived from the ideal cubic $Pm\bar{3}m$ structure by a combination of in-phase octahedral tilting about $\langle 001 \rangle_p$ and out-of-phase octahedral tilting about $\langle 110 \rangle_p$. The in-phase tilting is a consequence of the condensation of the M_3 soft mode while the out-of-phase tilts are due to condensation of the R_{25} soft mode. The larger Cd^{2+} cations occupy the cuboctahedral sites, although as a consequence of the tilting of the TiO_6 octahedra the Cd^{2+} cations are effectively eight coordinate with the other 4 Cd–O contacts being greater than 3.1 Å. The BVS for the Ti cation is 3.97 whilst that for the Cd cation suggests this is equally underbonded in both the perovskite and ilmenite structures, being 1.66. The refined structural parameters for the perovskite-type $CdTiO_3$ structure and associated interatomic distances are collected in Tables 4–6.

Variable temperature XRD studies of selected members in the $Cd_{1-x}Ca_xTiO_3$ series did not reveal any phase transitions associated with removal of the tilting of the octahedra below 900 °C. This is not surprising, since the tolerance factor for $CdTiO_3$ is slightly less than that for $CaTiO_3$ resulting in larger tilts at room temperature in $CdTiO_3$ and it is reasonable to expect that these will only be lost at higher temperatures than that seen for $CaTiO_3$ [10].

Table 4
Crystal structure data and refined atomic coordinates and atomic displacement parameters (multiplied by 100.0) for perovskite-type $CdTiO_3$ at room temperature. It was not possible to refine anisotropic displacement parameters for the Ti cation.

Name	Site	*x*	*y*	*z*	Ue × 100	
Cd	4*c*	0.0076(6)	0.5397(5)	1/4	1.08*	
Ti	4*a*	0	0	0	0.63(9)	
O1	4*c*	−0.0898(5)	−0.0273(5)	1/4	0.72*	
O2	8*d*	0.2001(4)	0.2972(4)	0.04815(28)	1.06*	
	U_{11}	U_{22}	U_{33}	U_{12}	U_{13}	U_{23}
Cd	1.10(15)	1.19(13)	0.95(14)	0.76(14)	0	0
O1	1.30(15)	0.68(14)	0.18(14)	0.16(12)	0	0
O2	1.05(8)	0.79(8)	1.35(11)	−0.33(10)	0.12(10)	0.07(8)

Table 5
Crystal structure data and refined atomic coordinates and atomic displacement parameters (multiplied by 100.0) for perovskite-type $CdTiO_3$ at 4 K. The structure was refined in space group $Pna2_1$. Attempts to refine anisotropic displacement parameters resulted in unstable refinements.

Name	Site	*x*	*y*	*z*	$U \times 100$
Cd	4*a*	0.4596(4)	0.2482(11)	0.0098(4)	0.37(4)
Ti	4*a*	0.0051(23)	0.0076(11)	0.0009(29)	0.20(8)
O1	4*a*	0.5293(4)	0.2468(12	0.5913(4)	0.36(4)
O2	4*a*	0.2101(8)	0.0475(7)	0.2974(13)	0.04(11)
O3	4*a*	−0.1941(9)	−0.0491(8)	−0.3023(16)	1.24(17)

Table 6
Selected interatomic distances and angles in the perovskite type structure of $CdTiO_3$ at room temperature and at 4 K.

	RT (*Pbnm*)	4 K ($Pna2_1$)
a (Å)	5.30689(13)	5.41814(10)
b (Å)	5.42239(14)	7.60606(15)
c (Å)	7.62000(21)	5.29726(9)
Vol (Å^3)	219.273(10)	218.304(7)
Cd–O(1)	2.405(4)	2.2492(26)
Cd–O(1) (Å)	2.405(4)	2.3921(27)
Cd–O(2) (Å)	2.2666(29) × 2	2.545(9)
Cd–O(2) (Å)	2.593(4) × 2	2.701(10)
Cd–O(2) (Å)	2.6757(27) × 2	2.284(9)
Cd–O(3) (Å)		2.232(10)
Cd–O(3) (Å)		2.617(10)
Cd–O(3) (Å)		2.649(11)
Ti–O(1) (Å)	1.9693(7) × 2	2.049(13)
Ti–O(1) (Å)		1.888(13)
Ti–O(2) (Å)	1.9688(22) × 2	1.947(15) × 2
Ti–O(2) (Å)	1.9647(20) × 2	
Ti–O(3) (Å)		1.985(15) × 2
Ti–O1–Ti (deg.)	150.64(16)	150.00(12)
Ti–O2–Ti (deg.)	149.34(12)	152.5(6)
Ti–O3–Ti (deg.)		145.9(6)

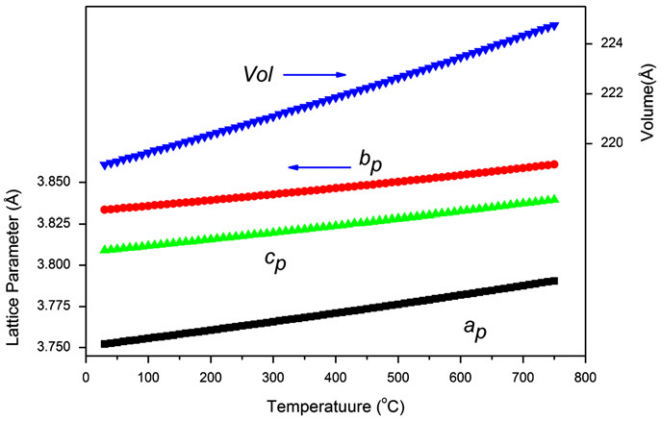

Fig. 3. Temperature dependence of the lattice parameters normalised to the perovskite subcell and unit cell volume for $CdTiO_3$ estimated from X-ray diffraction data. The error bars are smaller than symbols.

The temperature dependence of the lattice parameters for $CdTiO_3$, Fig. 3, is reminiscent of those for $CaMnO_3$ [27], which also remains orthorhombic in space group *Pbnm* over this temperature range, in that it approaches a metrically tetragonal cell whilst remaining orthorhombic. Similar effects have been observed in numerous other perovskites including $SrRuO_3$ [28,29] and $SrZrO_3$ [30], although both those ultimately transform to a cubic structure at elevated temperatures. Higher temperatures were not investigated here due to the potential loss of Cd.

Cooling the sample to 4 K did not result in the appearance of any additional reflections in the neutron diffraction pattern, nor was any additional splitting of the strongest Bragg reflections evident, even when using longer wavelength neutrons, see Fig. 2. The cell was clearly still orthorhombic and a satisfactory fit to the two neutron patterns (recorded with $\lambda=1.622$ and 2.442 Å) was obtained in *Pbnm* with $\chi^2=1.59\%$. The displacement parameters for each of the ions were unexceptional (provided an appropriate scattering length for the ^{114}Cd cations was employed). Space group *Pbnm* is, however, incompatible with the observed ferroelectric behaviour of $CdTiO_3$ at this temperature [6].

There are three possible space groups for the low temperature ferroelectric phase of $CdTiO_3$, and Rietveld refinements were conducted for all three. For both $P2_1ma$ and $Pnm2_1$ the resulting χ^2 was higher than that obtained in *Pbnm*, 1.73% and 1.71% respectively, which together with the presence of one, or more, negative displacement parameters suggest neither of these is the correct structure. The fit in $Pn2_1a$ provides the best agreement with the experimental data $\chi^2=1.56\%$ and the full refinement details, complete with isotropic displacement parameters are listed in Table 5. The BVS are 4.01 and 1.70 for Ti and Cd respectively. This conclusion is in agreement with the first-principles calculations of Lebedev [31] who concluded that the ground state of $CdTiO_3$the the ferroelectrically distorted $Pn2_1a$ phase.

The situation for $CdTiO_3$ is similar to, but not identical with, that of $NaNbO_3$. Rietveld refinements of neutron diffraction data

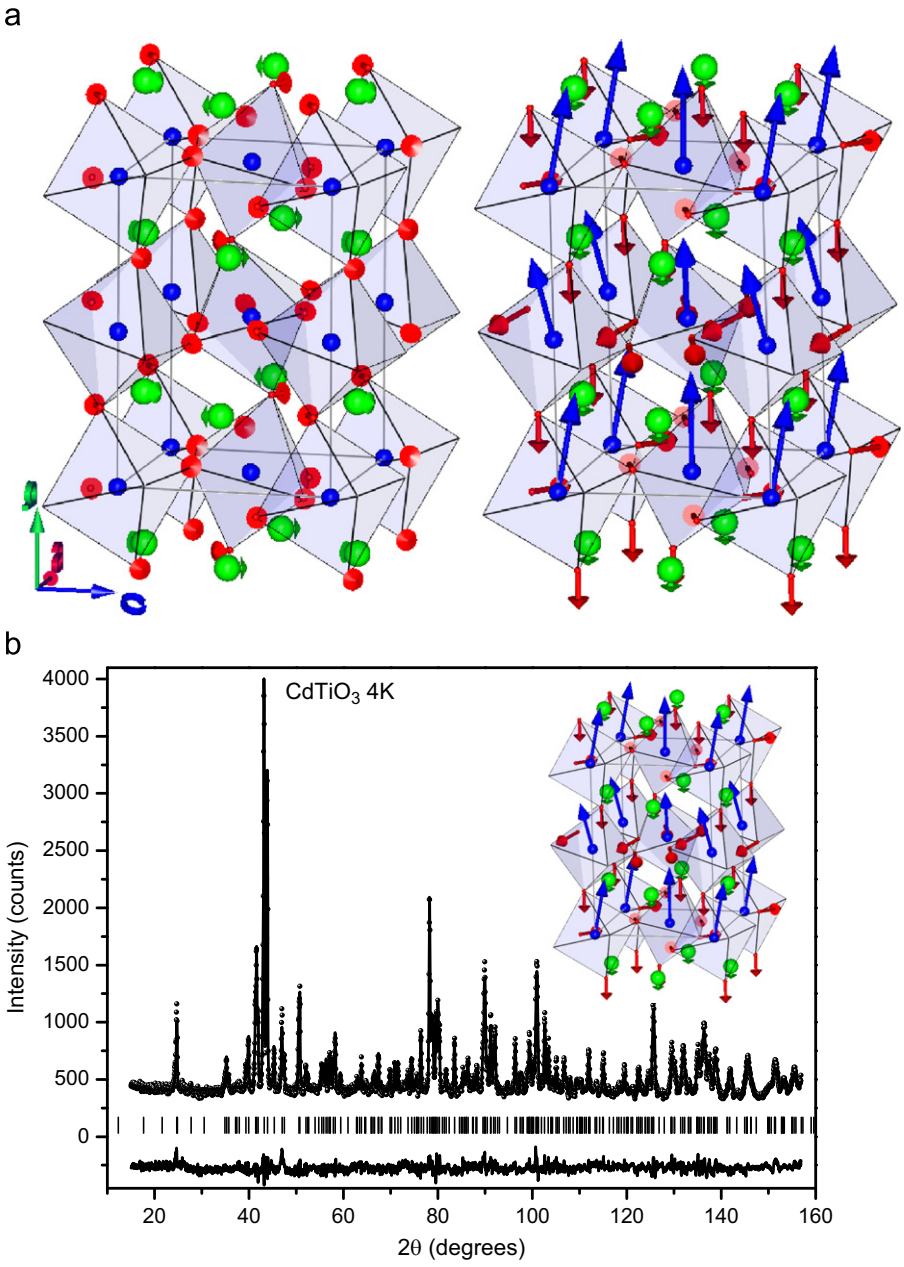

Fig. 4. Non-polar GM1+ (left) and polar GM4− (right) irrep distortions of the $Pn2_1a$ phase. Arrow lengths are proportional to the mode amplitudes.

for $NaNbO_3$ [32] suggested the ferroelectric phase was in $P2_1ma$ ($\chi^2=4.8$) with the $Pn2_1a$ model having a higher χ^2 value (5.6). Critically in the $Pn2_1a$ structure there is a single Na site whereas in $P2_1ma$ there are two distinct Na sites as was observed in NMR measurements [32]. Unfortunately we are unable to measure NMR spectra of $CdTiO_3$ below the transition temperature, although such measurements are clearly warranted. It may be significant that the polar structure in $CdTiO_3$ results from a second order $Pbnm \rightarrow Pn2_1a$ transition whereas in $NaNbO_3$ the polar $P2_1ma$ structure appears via a $Pbcm$ intermediate. We are unaware of any evidence for a $Pbcm$ phase in $CdTiO_3$. Whilst the subtle effects that differentiate the stability of these two polar structures are unknown, local bonding effects of the cations are presumably important. Raman studies have demonstrated that the substantially pure displacive second order transition in perovskite $CdTiO_3$ is driven by the softening of a soft mode [33]. Anomalies in the Raman spectra of the ferroelectric phase of $CdTiO_3$ suggest there may be local symmetry breakdown [33] as seen in other ABO_3 perovskites [34,35]. The local symmetry breakdown is believed to be induced by A–O bond disorder, and such small changes in the local symmetry may be sufficient to stabilise the $Pn2_1a$ structure with-respect to $P2_1ma$.

The distortion of the low-temperature ferroelectric $Pn2_1a$ phase with respect to the parent $Pbnm$ modification was explored in terms of symmetry-adapted modes using the AMPLIMODES code [36]. After shifting the unit cell origin along the polar b-axis by 0.00021 in order to eliminate global translation of the ferroelectric phase, the $Pn2_1a$ distortion was decomposed into two modes corresponding to the irreducible representations (irreps) GM1+ and GM4−. The amplitudes of the 7-dimensional non-polar GM1+ (isotropy subgroup $Pbnm$) and 8-dimensional polar GM4− (isotropy subgroup $Pn2_1a$) were found to be 0.0377 Å and 0.1889 Å, respectively, indicating that the latter is the primary distortion mode (Fig. 4).

Based on the individual atomic displacement and ionic formal charges we also estimated the spontaneous polarisation P_s using

$$P_s = \frac{\sum_i (m_i \Delta y_i Z_i) e}{V} \quad (1)$$

where m_i is the crystallographic site multiplicity, Δy_i is the displacement along the polar axis from the corresponding position in the paraelectric phase along the polar axis, $Z_i e$ is the ionic charge, and V is the unit cell volume. The calculated value 0.078 C/m^2 lies between that predicted by *ab initio* calculations (0.21 C/m^2) [31] and observed experimentally (0.009 C/m^2) [37].

3.4. Doping experiments

Solid solutions of the type $Cd_{1-x}Ca_xTiO_3$ could be prepared. Invariably this required the use of relatively high temperatures resulting in the formation of perovskite-type oxides and we did not find any evidence to suggest appreciable amounts of Ca could be incorporated into the ilmenite type $CdTiO_3$ structure. It can be imagined that doping $CdTiO_3$ would have a significant impact on the stability of the ferroelectric phase. However, we could not prepare solid solutions of the type $Cd_{1-x}Sr_xTiO_3$ using conventional methods. This is somewhat remarkable given the relative ease with which oxides of the type $Ca_{1-x}Sr_xTiO_3$ can be prepared [38] and suggests the A–O bonding is playing a significant, but poorly understood role in stabilising the oxides. There is ample evidence that altering the A-cation significantly alters the hybridisation between the B-site metal t_{2g} d states and the O π p orbitals.

It was possible to prepare solid solutions of the type $Cd_{1-x}Zn_xTiO_3$ with an ilmenite type structure. Single phase samples were obtained for small $x \leq 0.2$ or large $x > 0.8$ values of x. For other Zn:Cd ratios phase separation occurred and two separate rhombohedral phase of $ZnTiO_3$ and $CdTiO_3$ were present.

4. Conclusion

The structures of three phases of $CdTiO_3$ prepared using ^{114}Cd have been refined using powder neutron diffraction data. At room temperature $CdTiO_3$ adopts either an ilmenite or perovskite type structure depending on the preparative conditions. In both structures the Cd is slightly underbonded with an effective bond valence of around 1.7. The perovskite-form undergoes a transition to a ferroelectric structure upon cooling and the neutron data suggests this is to a second orthorhombic structure in space group $Pna2_1$ rather than the $P2_1ma$ structure observed in $NaNbO_3$. It was necessary to refine the neutron scattering length of the ^{114}Cd and this was estimated to be 5.56 fm.

Acknowledgments

BJK acknowledges the support of the Australian Research Council and the Australian Institute of Nuclear Science and Engineering for aspects of this work.

Appendix A. Supplementary materials

Supplementary data associated with this article can be found in the online version at doi:10.1016/j.jssc.2011.08.028.

References

[1] J.M. Neil, A. Navrotsky, O.J. Kleppa, Inorg. Chem. 10 (1971) 2076–2077.
[2] P.D. Sesion, J.M. Henriques, C.A. Barboza, E.L. Albuquerque, V.N. Freire, E.W.S. Caetano, J. Phys.: Condens. Matter 22 (2011) 435801.
[3] H. Wang, X. Zhang, A. Huang, H. Xu, M. Zhu, B. Wang, H. Yan, M. Yoshimura, J. Cryst. Growth 246 (2002) 150–154.
[4] E. Posnjak, T.F.W. Barth, Z. Kristallogr. 88 (1934) 271–280.
[5] S.A. Mayen-Hernandez, G. Torres-Delgado, R. Castanedo-Perez, J.G. Mendoza-Alvarez, O. Zelaya-Angel, J. Adv. Oxid. Technol. 10 (2007) 85–89.
[6] P.H. Sun, T. Nakamura, Y.J. Shan, Y. Inaguma, M. Itoh, Ferroelectrics 217 (1998) 137–145.
[7] A.M. Glazer, Acta Crystallogr. Sect. B—Struct. Commun. B 28 (1972) 3384 &.
[8] H.F. Kay, J.L. Miles, Acta Crystallogr. 10 (1957) 213–218.
[9] S. Sasaki, C.T. Prewitt, J.D. Bass, W.A. Schulze, Acta Crystallogr. Sect. C—Cryst. Struct. Commun. 43 (1987) 1668–1674.
[10] B.J. Kennedy, C.J. Howard, B.C. Chakoumakos, J. Phys.: Condens. Matter 11 (1999) 1479–1488.
[11] Y.J. Shan, H. Mori, K. Tezuka, H. Imoto, M. Itoh, Ferroelectrics 284 (2003) 281–286.
[12] G. Shirane, R. Pepinsky, B.C. Frazer, Acta Crystallogr. 9 (1956) 131–140.
[13] G.H. Kwei, A.C. Lawson, S.J.L. Billinge, S.W. Cheong, J. Phys. Chem. 97 (1993) 2368–2377.
[14] R. Ranjan, R.S.K. Mishra, D. Pandey, B.J. Kennedy, Phys. Rev. B 65 (2002) 4.
[15] W. Zhong, D. Vanderbilt, Phys. Rev. Lett. 74 (1995) 2587–2590.
[16] V.V. Lemanov, A.V. Sotnikov, E.P. Smirnova, M. Weihnacht, R. Kunze, Solid State Commun. 110 (1999) 611–614.
[17] K.D. Liss, B. Hunter, M. Hagen, T. Noakes, S. Kennedy, Physica B—Condens. Matter 385–386 (2006) 1010–1012.
[18] A.C. Larson, R.B. Von Dreele, Los Alamos National Laboratory Report, LAUR 86-748, 1994.
[19] B.H. Toby, J. Appl. Crystallogr. 34 (2001) 210–213.
[20] R.C. Liebermann, Earth Planet. Sci. Lett. 29 (1976) 326–332.
[21] M.R. Mohammadi, D.J. Fray, Acta Mater. 57 (2009) 1049–1059.
[22] A.R. Phani, M. Passacantando, S. Santucci, J. Mater. Sci. 35 (2000) 5295–5299.
[23] F.H. Dulin, D.E. Rase, J. Am. Ceram. Soc. 43 (1960) 125–131.
[24] Y.S. Chang, Y.H. Chang, I.G. Chen, G.J. Chen, Y.L. Chai, T.H. Fang, S. Wu, Ceram. Int. 30 (2004) 2183–2189.
[25] V.F. Sears, Neutron News 3 (1992) 29–37.
[26] R.D. Shannon, Acta Crystallogr. Sect. A 32 (1976) 751–767.
[27] Q.D. Zhou, B.J. Kennedy, J. Phys. Chem. Solids 67 (2006) 1595–1598.
[28] B.J. Kennedy, B.A. Hunter, J.R. Hester, Phys. Rev. B 65 (2002) 4.
[29] B.J. Kennedy, B.A. Hunter, Phys. Rev. B 58 (1998) 653–658.

[30] C.J. Howard, K.S. Knight, B.J. Kennedy, E.H. Kisi, J. Phys.: Condens. Matter 12 (2000) L677–L683.
[31] A.I. Lebedev, Phys. Solid State 51 (2009) 802–809.
[32] K.E. Johnston, C.C. Tang, J.E. Parker, K.S. Knight, P. Lightfoot, S.E. Ashbrook, J. Am. Chem. Soc. 132 (2010) 8732–8746.
[33] H. Taniguchi, Y.J. Shan, H. Mori, M. Itoh, Phys. Rev. B 76 (2007) 212103.
[34] B. Zalar, V.V. Laguta, R. Blinc, Phys. Rev. Lett. 90 (2003) 037601.
[35] R. Blinc, B. Zalar, V.V. Laguta, M. Itoh, Phys. Rev. Lett. 94 (2005) 147601.
[36] D. Orobengoa, C. Capillas, M.I. Aroyo, J.M. Perez-Mato, J. Appl. Crystallogr. 42 (2009) 820–833.
[37] M.E. Guzhva, V.V. Lemanov, P.A. Markovin, Phys. Solid State 43 (2001) 2146–2153.
[38] C.J. Ball, B.D. Begg, D.J. Cookson, G.J. Thorogood, E.R. Vance, J. Solid State Chem. 139 (1998) 238–247.